Journal of Biomechanics 94 (2019) 211–218

Contents lists available at ScienceDirect

Journal of Biomechanics

journal homepage: www.elsevier.com/locate/jbiomech
www.JBiomech.com

Effect of variable periodontal ligament thickness and its non-linear material properties on the location of a tooth's centre of resistance

Falko Schmidt *, Bernd Georg Lapatki

Department of Orthodontics, Centre of Dentistry, University of Ulm, Albert-Einstein-Allee 11, 89081 Ulm, Germany

ARTICLE INFO

Article history:
Accepted 31 July 2019

Keywords:
Centre of resistance
Orthodontic tooth movement
Finite element method
FE model
PDL model
Non-linear material

ABSTRACT

In orthodontics, the 3D translational and rotational movement of a tooth is determined by the force–moment system applied and the location of the tooth's centre of resistance (CR). Because of the practical constraints of in-vivo experiments, the finite element (FE) method is commonly used to determine the CR. The objective of this study was to investigate the geometric model details required for accurate CR determination, and the effect of material non-linearity of the periodontal ligament (PDL). A FE model of a human lower canine derived from a high-resolution μCT scan (voxel size: 50 μm) was investigated by applying four different modelling approaches to the PDL. These comprised linear and non-linear material models, each with uniform and realistic PDL thickness. The CR locations determined for the four model configurations were in the range 37.2–45.3% (alveolar margin: 0%; root apex: 100%). We observed that a non-linear material model introduces load-dependent results that are dominated by the PDL regions under tension. Load variation within the range used in clinical orthodontic practice resulted in CR variations below 0.3%. Furthermore, the individualized realistic PDL geometry shifted the CR towards the alveolar margin by 2.3% and 2.8% on average for the linear and non-linear material models, respectively. We concluded that for conventional clinical therapy and the generation of representative reference data, the least sophisticated modelling approach with linear material behaviour and uniform PDL thickness appears sufficiently accurate. Research applications that require more precise treatment monitoring and planning may, however, benefit from the more accurate results obtained from the non-linear constitutive law and individualized realistic PDL geometry.

© 2019 Elsevier Ltd. All rights reserved.

1. Introduction

The objective of orthodontic therapy is to correct malocclusion and the malposition of individual teeth. Orthodontic tooth movement (OTM) is achieved by remodelling the alveolar bone, i.e. bone deposition and resorption at opposite sides of the root. Such remodelling is stimulated by therapeutic loads initiating cascades of biological processes (Meikle, 2005). Despite the complexity of the underlying biological and mechanical systems, the extent of OTM can be approximated by incremental consideration of initial tooth movement (ITM) (Bourauel et al., 2000). ITM is dominated by the instantaneous load reaction caused by the viscoelastic compliance of the thin layer of connective tissue between the tooth root and alveolar bone, called the periodontal ligament (PDL). The interrelationship between the mechanical load components and the type of OTM, i.e. translation and/or rotation achieved in three-dimensional (3D) space, can be described on the basis of the centre of resistance (CR).

The CR is defined as the point at which the application of a pure force would result in a purely translational ITM (Burstone, 1962; Burstone and Pryputniewicz, 1980; Osipenko MA. et al., 1999). This point is naturally located in the embedded part of the root and is therefore not directly accessible for the application of therapeutic loads. Consequently, in the common clinical situation of load application via an orthodontic bracket bonded to the labial crown surface, a combined force and moment application with a specific ratio is required to achieve such a purely translational ITM. The respective moment-to-force ratio corresponds to the distance between the bracket slot and the CR. More generally speaking, the translational and rotational proportions of 3D OTM depend on the quantitative interrelationship of the 3D force and moment components exerted by the orthodontic appliance on the individual teeth.

In addition to above-mentioned geometric variables, the CR location also depends on the direction of movement (Dathe et al., 2013; Meyer et al., 2010) and mechanical PDL properties.

* Corresponding author.
E-mail address: falko.schmidt@uni-ulm.de (F. Schmidt).

https://doi.org/10.1016/j.jbiomech.2019.07.043
0021-9290/© 2019 Elsevier Ltd. All rights reserved.

(Nyashin et al., 2015). Most variables have high inter-individual variability, as shown by previous anatomical and experimental studies (Brook et al., 2009; Cronau et al., 2006; Garn et al., 1968; Keilig et al., 2015; Peck and Peck, 1972; Schumacher, 1983). This variability includes pathological conditions such as periodontitis, which reduces the attachment of the PDL to the root surface due to loss of alveolar bone (Geramy, 2000; Kettenbeil et al., 2013; Towfighi et al., 1997).

Finite element (FE) analysis has been widely employed to investigate OTM and the related mechanical behaviour of the PDL (Cattaneo et al., 2008; Dorow, 2004; Geiger and Lapatki, 2014; Geramy, 2000; Jones et al., 2001; Meyer et al., 2010; Nikolaus et al., 2017; Tanne et al., 1988; Vollmer et al., 1999). Assessment of the CR's location using numerical methods has been based on geometric simplifications such as uniform PDL thickness (Kojima and Fukui, 2014; Provatidis, 2000), a somewhat coarse geometric resolution (Meyer et al., 2010; Vollmer et al., 1999) or unrealistic linear material models (Geramy, 2000; Viecilli et al., 2013), or a combination of these (Dathe et al., 2013; Nyashin et al., 2015; Provatidis, 1999). It has been suggested that the PDL is hourglass-shaped (Coolidge, 1937; Toms and Eberhardt, 2003) and its thickness varies locally due to uneven alveolar bone surfaces (Boryor et al., 2009; Dalstra et al., 2006). Furthermore, it has been observed that PDL material non-linearity affects the distribution of mechanical stresses generated by ITM (Nikolaus et al., 2017; Qian et al., 2001; Toms and Eberhardt, 2003) and, thus, the CR location (Nyashin et al., 2015).

To the best of our knowledge, no studies have considered both biofidelic PDL geometry and non-linear material behaviour in relation to the location of the CR. Hence, the objective of this study was to quantify the effect of the following variables on CR location for a human lower canine: (1) simplified modelling (i.e. a layer of uniform thickness) vs. accurate modelling (i.e. realistic representation characterized by a variable thickness) of the PDL geometry and (2) linear vs. non-linear PDL material description. Moreover, the effects of load direction and magnitude on the CR location were examined for four tooth movements commonly considered in orthodontics, i.e. in the mesial, distal, buccal and lingual directions.

2. Materials and methods

2.1. Morphological tooth model

This study used a highly accurate geometric model of a human lower canine (Fig. 1) that had been established in a previous study (Boryor et al., 2009). A section of the mandible that includes the sample tooth and surrounding bone was cut from a 79-year-old cadaver and stored in 70% alcohol solution before being scanned with a voxel size of 50 μm using microcomputed tomography (μCT). The anatomical orientation of the tooth model, i.e. its inclination and angulation relative to a virtual plane between the upper and lower dental arches (the so-called occlusal plane) (Geiger and Lapatki, 2014), was chosen according to a widely accepted fundamental orthodontic study (Andrews, 1972). The same reference frame was used for a direction-dependent analysis of the PDL thickness distribution.

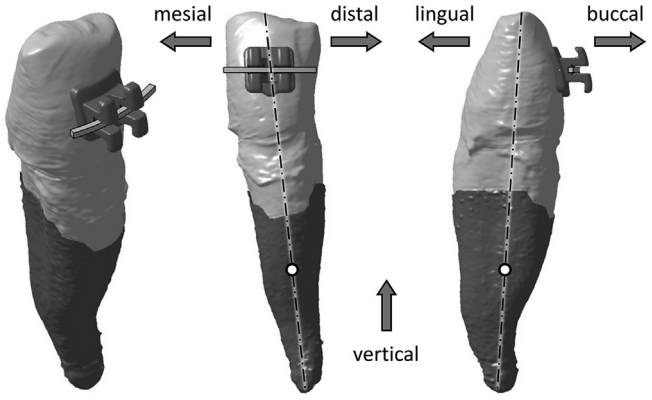

Fig. 1. Images of the tooth with periodontal ligament positioned according to mean inclinations established by Andrews (1972), with identification of the directions as used by orthodontists (buccal, lingual, mesial and distal), the tooth axis (dot-and-dashed line) and an averaged CR (white marker).

2.2. FE modelling

Four different FE models were created and solved using commercial software (Abaqus; Version 6.11, Dassault Systèmes). They shared the same tooth mesh but had different combinations of a linear or non-linear description of PDL material behaviour and a uniform or realistic representation of PDL width distribution.

For the linear material model (Fig. 2), the PDL was considered homogenous, isotropic, linear-elastic and time-independent. This was implemented using the conventional generalized Hooke's law with a Young's modulus of 0.1 MPa and a Poisson's ratio of 0.45 (Dorow and Sander, 2005; Geiger and Lapatki, 2014). In contrast, the non-linear material description is based on a model proposed by Cattaneo et al. (2005). Although the PDL's macroscopic behaviour is modelled in an isotropic manner it reflects the microscopic structure of the PDL. A collagen network dominates the PDL stiffness under tensile loading. Under compression, this network lacks structural resistance. Additionally, the substantial amount of liquid contained in the extracellular matrix and vascular network shifts from compressed to expanded PDL regions. Hence, when quasi-static conditions are considered the PDL provides only limited stiffness under a wide range of compression conditions. The combined material response of the different constituents was described with a non-linear stiffness characteristic as depicted in Fig. 2. It has to be noted, however, that the applied model does not account for anisotropic behaviour caused by the predominant orientation of the collagen fibres. The volumetric behaviour was governed by a Poisson's ratio of 0.3, which is in accordance with

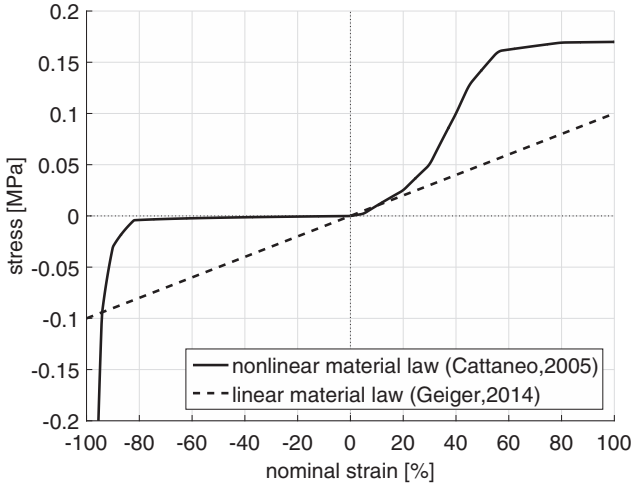

Fig. 2. Stress–strain curves for the linear and non-linear material laws applied. The non-linear constitutive law (solid line) is based on Cattaneo et al. (2005) but has been approximated by multiple linear regimes. The graph depicted was created from results of a finite element analysis simulating a tension-compression experiment with a unit cube using the strain-dependent tangent moduli given in the table. The linear material law (dashed line) refers to Geiger and Lapatki (2014), who applied a Young's modulus E = 0.1 MPa and Poisson's ratio ν = 0.45.

Cattaneo et al. (2005). As the applied FE software did not provide an adequate material model to reproduce this behaviour, a user-defined constitutive law was implemented using an elastic multilinear description. The elastic modulus of bone and dental hard tissue differs from that of the PDL by approximately 4–5 orders of magnitude (Dong-Xu et al., 2011; Kinney et al., 2003; O'Mahony et al., 2001; Papadopoulou et al., 2013; Schwartz-Dabney and Dechow, 2003; Yoshida et al., 2001). Hence, bone and dental hard tissue were assumed to be rigid in all four models. An overview of the model parameters is given in Table 1.

Geometric representation of a realistic PDL layer, which is characterized by a variable thickness, was derived by means of segmentation and was meshed using linear tetrahedrons sharing the nodes of the tooth mesh at the interface. In contrast, the uniform PDL mesh with a uniform layer thickness of 250 μm was created using normal offsets of the bone–PDL interface surface elements, which resulted in four layers of triangular prism elements. To reduce the number of nodes and, consequently, computational costs, only the outer shape of the tooth was represented using rigid triangular linear shell elements, based on the assumption of its rigidity.

Modelling of the rigid alveolar bone was omitted by fixing the geometric position of the interface nodes of the bone and PDL. Simulations were driven by predefined displacements of the tooth mesh in the direction being considered (mesial, distal, buccal or lingual). Because of the rigid formulation, reaction forces and moments could be evaluated at a single point. This reference point (RP) was defined as the centre between the most cervical extensions of the mesial and distal alveolar margins. The RP was located 7.65 mm below the load application point, i.e. the centre of the bracket slot, specified according to Andrews (1972). All numerical computations in this study were run on a local desktop machine.

2.3. Location of CR

To ensure lack of ambiguity, the CR was defined as the point on the line of action of a pure force causing a purely translational movement in a predefined direction that is closest to the tooth axis. The tooth axis (Fig. 1) was defined as the line crossing the most incisal point in the mesio-distal centre of the labial crown surface and the most prominent point at the apex. From the total reaction forces $\overrightarrow{F_R}$ and moments $\overrightarrow{M_R}$ generated by a tooth displacement with respect to the point RP, the respective relative position $\overrightarrow{l_{CR}}$ of the pure force vector crossing the CR was obtained using the relationship

$$\overrightarrow{M_R} = \overrightarrow{l_{CR}} \times \overrightarrow{F_R}. \quad (1)$$

A least-square solver (Matlab; version R2015b, The MathWorks Inc.) was used to find a unique solution fulfilling the aforementioned condition. The CR location was finally evaluated in the vertical direction as the distance from the reference point (RP). This distance was also normalized in relation to the height of the embedded root, defined as the vertical distance from the RP at the alveolar margin (0%) to the root apex (100%).

3. Results

3.1. PDL thickness

The vertical and circumferential distributions of the PDL width of the realistic model are given in Fig. 3. In most cases, the PDL width ranges between 59 μm and 407 μm, with a median value of approximately 100 μm in most regions. In the vertical direction (Fig. 3A), the graph of median PDL thickness derived over the corresponding circumference increases to approximately 150–200 μm in the apical region. In contrast, the mean thickness of the cervical and middle regions of the root is almost constant, with a small peak of 156 μm at the cervical alveolar margin. Fig. 3B shows that a prominent circumferential dependency of the PDL width cannot be identified. Regions of slightly increased thickness are located at 0° and 90°, however, corresponding to the mesio-buccal and disto-buccal directions, respectively. In the lingual direction, the PDL layer generally seems thinner, with median thickness minima at 194° and 248°.

The local width variation depicted in Fig. 4 shows that the two extreme values in the lingual and buccal directions relate to vertical grooves and ridges in the upper part of the root. The cervical PDL margin is vertically located in a narrow range of ±0.27 mm from the reference height level on the distal and mesial sides, but reduces to −0.72 mm and −2.07 mm on the lingual and buccal sides, respectively.

3.2. Location of CR for the different FE models

Fig. 5 depicts CR locations in the vertical direction with respect to the RP at the alveolar margin obtained by use of the four modelling approaches for the bucco-lingual (Fig. 5A) and mesio-distal (Fig. 5B) loading directions. Most CR values ranged between −5.02 mm (37.2%) and −6.11 mm (45.3%).

Linear material modelling resulted in CRs that were load-independent and equal for opposing load directions. For the most simplified PDL model with linear material and uniform width, a CR location was found at a height of −5.80 mm (43.0%) in the bucco-lingual direction and at −5.39 mm (40.0%) in the mesio-distal direction. Using the realistic PDL geometry, more cervical CR locations were obtained at −5.46 mm (40.5%) and −5.12 mm (38.0%) in the bucco-lingual and mesio-distal directions, respectively.

Results generated using the non-linear material model were different for all directions and exhibited certain fluctuations within the load range considered. Changes in the CR location were most prominent for load magnitudes below 0.3 N. Above this magnitude, variations generally reduced to approximately 0.10 mm (0.76%). In this region, i.e. for loads above 0.3 N, mean CR locations of −5.62 mm (41.7%), −5.61 mm (41.6%) , −6.08 mm (45.1%) and −5.45 mm (40.4%) were found for loading in the buccal, distal, lingual and mesial directions, respectively, if the PDL is approximated by a uniform layer. For the most sophisticated model with non-linear material and realistic PDL geometry, the corresponding

Table 1
Overview of parameter of finite element models.

Model		Material	Nodes	Elements	Element type
Tooth		Rigid	133,499	266,994	Linear triangular shell
PDL	Uniform layer thickness	Linear E = 0.1 MPa, ν = 0.45 Non-linear acc. to Cattaneo et al. (2005, Fig. 2)	268,910	428,648	Linear triangular prisms
	Realistic variable layer thickness	Linear E = 0.1 MPa, ν = 0.45 Non-linear acc. to Cattaneo et al. (2005, Fig. 2)	1,147,066	250,055	Linear tetrahedrons

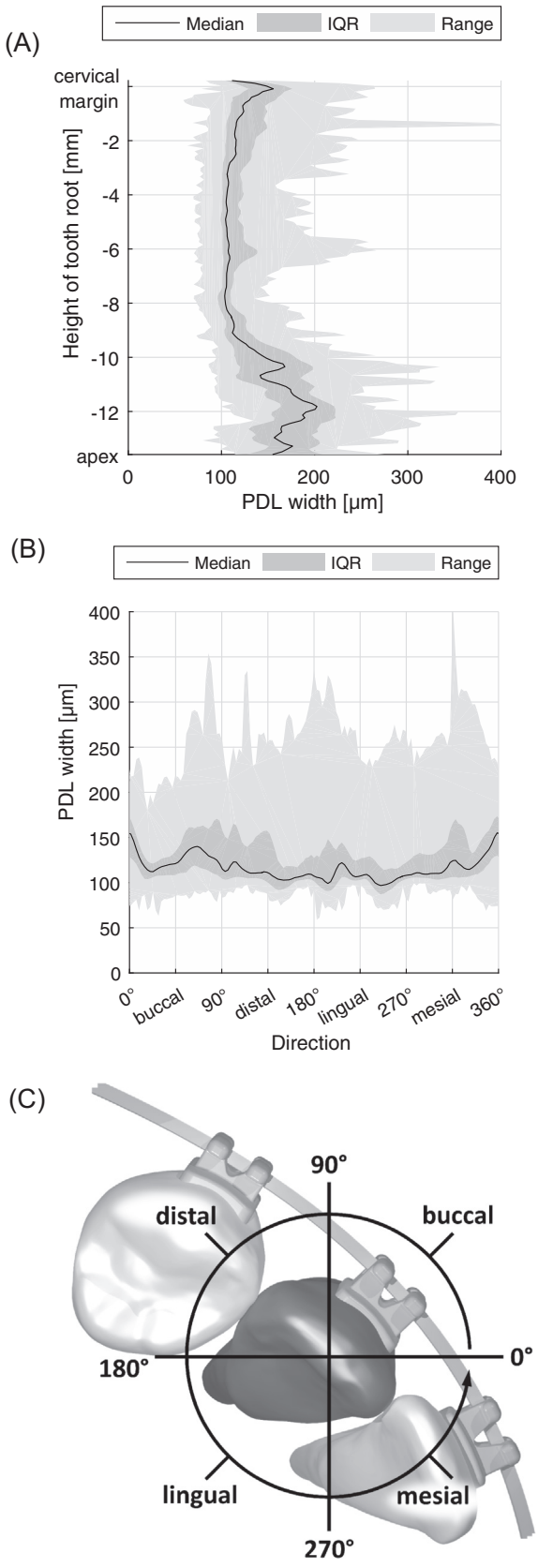

Fig. 3. Vertical (A) and circumferential (B) distribution of the PDL width. The median value (solid line), inter-quartile range (grey area) and total range (light-grey area) were derived from the closest point distance between the PDL–bone interface (58639 vertices) and the outer shell of the tooth (133499 vertices). The tooth segment (C) indicates the circumferential directions used in B.

mean values are −5.10 mm (buccal; 37.8%), −5.32 mm (distal; 39.4%), −5.85 mm (lingual; 43.4%) and −5.10 mm (mesial; 37.8%). The assumption of a uniform PDL thickness generally shifts the CR location towards the apex of the tooth root in a range of approximately 0.23 mm (1.7%, non-linear material model, lingual ITM) to 0.52 mm (3.9%, non-linear material model, buccal ITM).

4. Discussion

FE modelling is the preferred method for estimating CR locations of individual human teeth. Although in-vivo measurement systems for CR locations have been proposed (Yoshida et al., 2000), their application is highly limited because interproximal contacts between teeth usually restrict the ITM required, resulting in invalid CR locations. Furthermore, results only apply to the tooth examined, and it is difficult to determine correlations with individual characteristics. In contrast, the FE approach enables investigation of the effect of individual variables on CR location. This study used two variables that are inherent in the PDL, i.e. uniform vs. realistic thickness and linear vs. non-linear material behaviour.

Particularly notable are the large fluctuations in CR location within the load path introduced by the non-linear material model for both the simplified PDL layer with uniform thickness and the realistic representation which is anatomically accurate. The major changes close to the load-free state result from the striking dominance of overall mechanical behaviour by PDL regions under tension, because the material law applied assumes negligible stiffness for a wide range in the compression region. The greatest changes for very small loads are related to the gradual increase in stiffness for small strains. For larger loads, the CR then stabilizes to a different level for each direction. This level relates to the height of the PDL margin (which reflects the amount the tooth is embedded) on the tension side, which predominantly varies in the bucco-lingual direction, but to a minor extent also in the mesio-distal direction. In theory, another potentially major change in CR location must be expected for very large loads. This is because a dramatic increase in PDL stiffness for large compressional strains shifts the mechanical dominance to the pressure side. In such a situation, the hard tissues, i.e. bone and tooth root, would be close to direct contact. However, this load level could not be achieved in our simulations because of numerical instabilities for very large deformations.

The local variability of the thickness of the biofidelic (i.e. realistic) PDL layer is high because of cavities in the alveolar bone surface. Despite this, the lower canine investigated was generally characterized by a predominantly thin PDL layer in the cervical two thirds of the root height. Simulation results indicated larger strains in the latter cervical region, leading to the transmission of a greater proportion of the load in this region compared with the apical region with a thicker PDL. This causes the CR to shift towards the tooth crown. Load independence was preserved for the linear material model, whereas the extent of fluctuations increased when the non-linear constitutive law was applied. In the latter case, an increased load is inhibited by the thin layered regions on the tension side, an effect which can even be amplified by the progressive increase of the tensile stiffness up to 50% strain, due to successive engagement of collagen fibres.

To illustrate this interrelationship, Fig. 6 shows the vertical distribution of the realistic PDL geometry on the tension side and the associated CR location for the distinct load directions. Data are depicted for the most sophisticated modelling approach incorporating the non-linear material model. Two effects can be clearly recognized. First, if the cervical bone margin is recessed on one side, a reduction occurs in the height of the tooth's embedding in

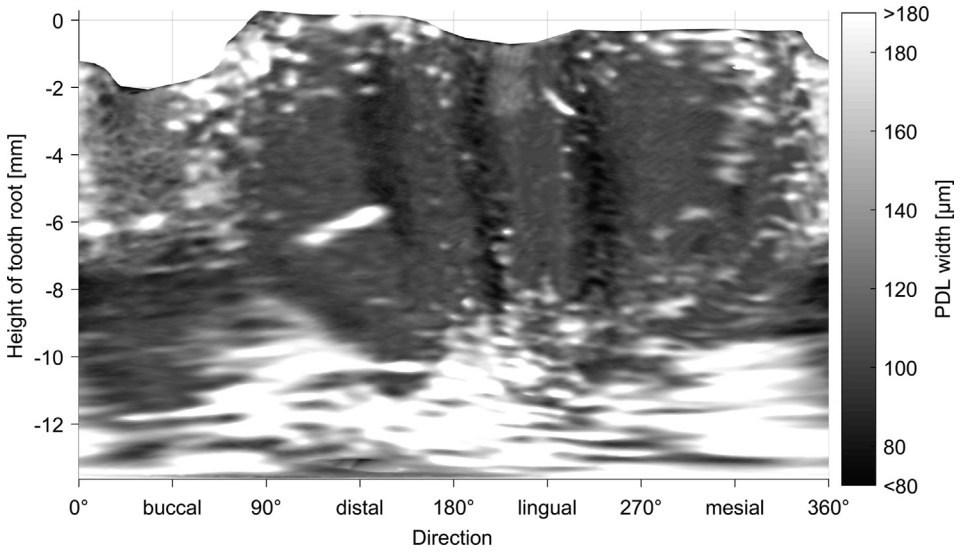

Fig. 4. Map of local PDL width generated by cylindrical projection. Dark areas indicate thin PDL regions whereas white indicates regions with a larger gap between hard tooth substance and alveolar bone.

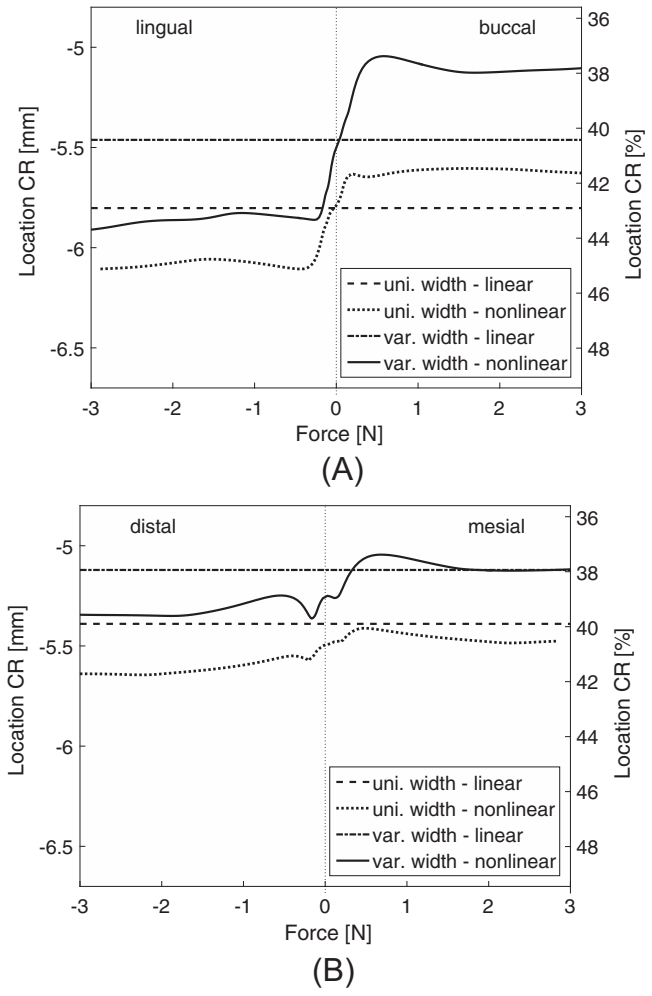

Fig. 5. Graphs of the location of the centre of resistance (CR) in the vertical direction derived for loading in the bucco-lingual (A) and mesio-distal (B) directions and depending on force magnitude. Data are given for the model with uniform PDL thickness governed by Hooke's law (dashed line) and using the non-linear material model (dotted line) based on Cattaneo et al. (2005) (Fig. 2), and for the model with variable PDL thickness as derived from a µCT scan with the same linear (dot-and-dashed line) and non-linear (solid line) material description.

the alveolar bone and, thus, the effective root length. Consequently, for loading in the opposite direction, the CR is shifted apically. Second, the respective CR tends to shift towards regions in which the gaps between the alveolar bone and the root are narrowest, because the PDL provides an increased supporting effect there, amplified by the progressive material stiffness. Most noticeably, the two effects enhance each other in the PDL on the buccal side (Fig. 6A) and are less pronounced on the mesial side (Fig. 6D). As a result, CR locations are found more apical than ITM dominated by the PDL on the distal (Fig. 6B) and lingual (Fig. 6C) sides. On the distal and lingual sides the two mechanisms counteract one another such that the CR locations obtained are almost identical.

From a more general perspective, the CR locations determined by the four different PDL modelling approaches are in good agreement with those of previous studies investigating lower canines. For example, Bourauel et al. (2007) proposed CR locations of 43% and 36.5% in the bucco-lingual and mesio-distal directions, respectively, assuming bi-linear PDL behaviour. An earlier study reported values in the range of 36–48% for five specimens, with almost identical results for all load directions (Poppe et al., 2002). Neither study, however, took into account the different mechanical behaviour of the PDL under pressure and tension caused by its multiphasic fibre-reinforced structure. The latter study also disregarded the variable height of bone embedding.

Most variations found for the CR locations occurred at very low load levels that are below the values targeted for clinical treatment. Above 0.3 N, the CR locations stabilize such that variations can be considered negligible in a clinically relevant load range that we assume to be 0.5–1 N. If biofidelic PDL geometry and material non-linearity are treated separately, CR location changes by up to 0.34 mm (2.52%) and 0.30 mm (2.25%), respectively, for all directions compared with the results for the conventional approach assuming uniform PDL width and linear material behaviour. Taking into account both modelling parameters, the deviations obtained increase up to 0.76 mm (5.62%) for the sample tooth in this study. Hence, the errors generated by both simplifications are within the range of inter-individual variations (Geiger and Lapatki, 2014; Poppe et al., 2002) and should be admissible for most applications in the scope of conventional clinical therapy. However, some recent developments in orthodontics concerning the monitoring of OTM (Schmidt et al., 2018) and direct measurement of forces applied for each individual tooth (Lapatki and Paul, 2007) might

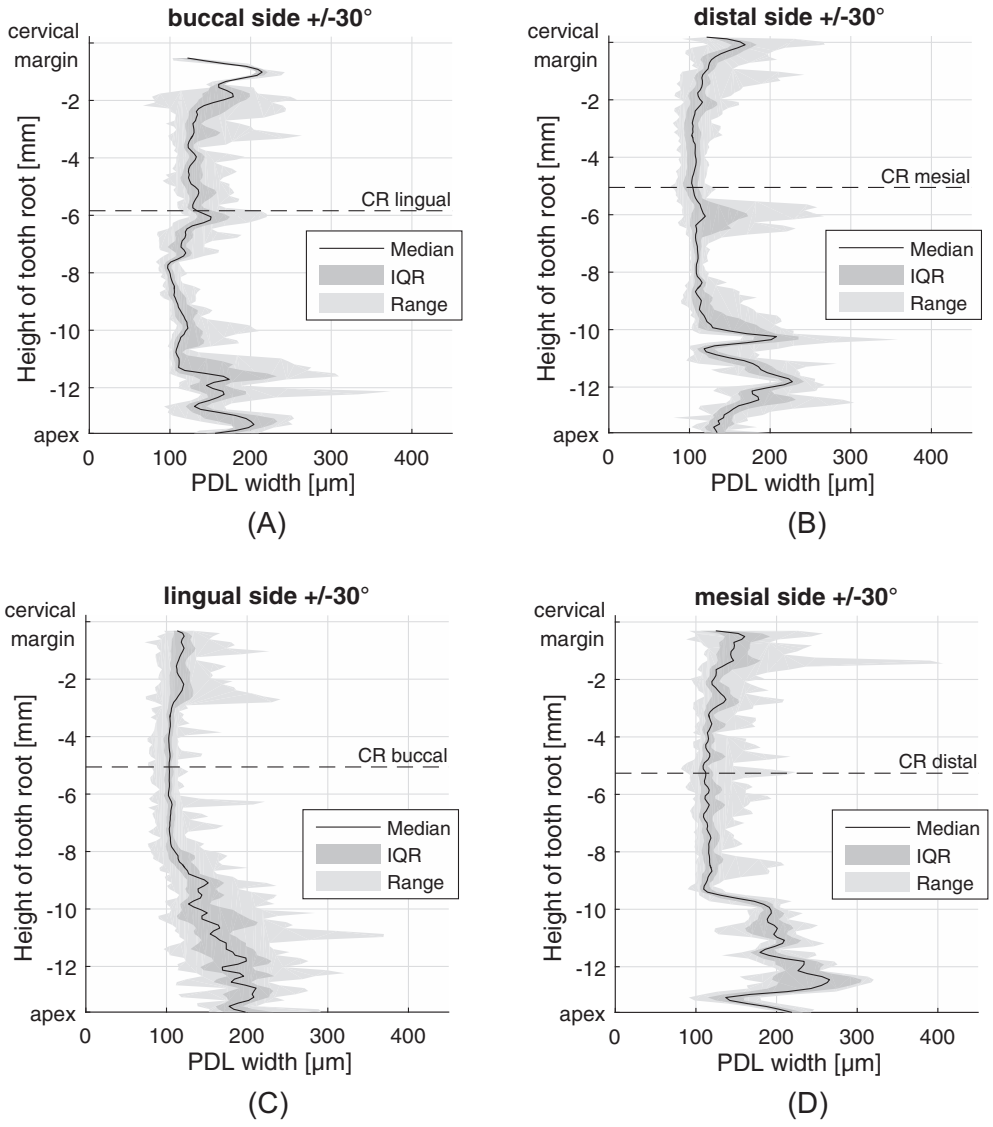

Fig. 6. Distribution of the PDL width in the vertical direction. Each graph includes regions within circumferential segments with a central angle of 60° spreading symmetrically around the buccal (A), distal (B), lingual (C) and mesial (D) directions. The median value is represented by a solid line whereas grey and light grey areas enclose the inter-quartile range (IQR) and overall range, respectively. The dashed line indicates the average location of the centre of resistance (CR) derived from the model with realistic PDL geometry and non-linear material description in a clinical load regime (0.5–1 N) to the opposite direction, i.e. when the dominating tensile stresses arise inside the circumferential PDL segment analysed.

enable more accurate treatment planning in future. Such developments might therefore benefit from more accurate, individualized CR locations.

Only a single tooth was examined in the present study because of the limited availability of sufficiently detailed models and the time consuming modelling procedure. Due to high morphological and biological variability, quantitative results presented cannot easily be applied to other individuals or tooth types. However, the study provides insights into mechanisms of how the variables within the scope of this study change the CR location and indicates a potential range of variability. Therefore, our exemplary results give valuable information about reasonable modelling approaches for future studies, e.g. to generate representative quantitative data on CR locations. Furthermore, the PDL width found for the tooth specimen investigated is somewhat thinner than the typical range of 150–380 µm specified in literature (Nanci and Cate, 2013,p 220). This could be explained by the age of the donor, but may also indicate that the tooth was non-functional (Coolidge, 1937). In addition, the PDL cross section did not have the almost symmetric hourglass shape found by others (Coolidge, 1937; Toms and Eberhardt, 2003). The thinnest PDL portion of the tooth specimen extends from the middle to the cervical third of the tooth root height and no distinctive thickness increase exists towards the cervical margin. The shift of the CR location should be less pronounced for a tooth with an hourglass-like PDL shape than that found in this study. Moreover, the actual thickness of the vertical grooves on the lingual side of the tooth root may not be resolved correctly because their dimensions are in the range of the voxel size of the scan. This might limit the accuracy of the results, especially for the CR location during buccal ITM. The transferability of our results to clinical application may also be limited by the age of the donor and the long period of specimen storage after extraction.

This study is further restricted to ITM in the elastic range of the PDL. Bourauel et al. (2000), however, successfully simulated OTM by iteratively analysing ITM based on the CR. Moreover, only four load directions were investigated. It should be noted in this respect that, although a greater range of variation might exist for other directions, the directions analysed are of particular interest to

orthodontists and are usually related to typical treatment tasks. Further limitations might be related to the applied material model. This issue is generally subject to ongoing debate and research. Very sophisticated material models have been proposed that incorporate visco-elasticity (Natali et al., 2008) as well as the direction-dependent influence of collagen fibres (Provatidis, 2000; Zhurov et al., 2007). Although the required mathematical foundation exists, there is still a demand for reliable experimental data to characterize the PDL in its full complexity. Because we are interested in the overall behaviour of the PDL in a steady-state, which is usually attained after approximately five hours of constant loading, disregarding visco-elasticity, time dependency and non-homogeneity was considered acceptable (Cattaneo et al., 2005). It has to be mentioned that the location of a tooth's CR may also be affected by the mechanical compliance of the alveolar bone which has not been considered in the applied model. Hohmann et al. (2011), however, investigated rigid and realistic bone modelling and could not find significant differences in the overall stress characteristics in the PDL (which are decisive for the CR). Hence, we suppose that alveolar bone compliance has only a minor impact on the CR location in the scope of this study.

5. Conclusion

In clinical practice, the CR provides an easy-to-use concept for estimation of OTM in orthodontic treatment planning. Deviations of CR location due to PDL width variation and material non-linearity were in an acceptable range for conventional therapeutic tasks. Hence, we recommend the simplified modelling approach with a uniform PDL layer and linear material characteristics for future FE studies conducted to generate representative reference data or for the estimation of CR locations of specific teeth for individual clinical applications. The main advantages of simplified PDL modelling are short computation times and the possibility of using standard volumetric scans. More accurate and individualized specifications of the CR location would, however, be beneficial for research purposes and for sophisticated treatment monitoring that requires enhanced precision. Here, the non-linear material behaviour should be considered to include potential load direction dependency. With regard to the advisability of geometrically exact modelling of the PDL layer, further research is required to determine typical patterns of PDL width variation. This will finally answer the question of its potential effect on CR location for use in clinical applications.

Declaration of Competing Interest

We declare that this article is free from conflicts of interest

Acknowledgements

We thank Hazel Davies, copy-editor, for English language revision.

Appendix A. Supplementary material

Supplementary data to this article can be found online at https://doi.org/10.1016/j.jbiomech.2019.07.043.

References

Andrews, L.F., 1972. The six keys to normal occlusion. Am. Jo. Orthod. 62, 296–309.
Boryor, A., Hohmann, A., Geiger, M., Wolfram, U., Sander, C., Sander, F.G., 2009. A downloadable meshed human canine tooth model with PDL and bone for finite element simulations. Dent. Mater.: Offi. Publ. Acad. Dent. Mater. 25, 62.
Bourauel, C., Keilig, L., Rahimi, A., Reimann, S., Ziegler, A., Jäger, A., 2007. Computer-aided analysis of the biomechanics of tooth movements. Int. J. Comput. Dent. 10, 25–40.
Bourauel, C., Vollmer, D., Jäger, A., 2000. Anwendung von Bone-Remodeling-Theorien zur Simulation orthodontischer Zahnbewegungen. J. Orofacial Orthopedics/Fortschritte der Kieferorthopädie 61, 266.
Brook, A.H., Griffin, R.C., Townsend, G., Levisianos, Y., Russell, J., Smith, R.N., 2009. Variability and patterning in permanent tooth size of four human ethnic groups. Arch. Oral Biol. 54 (Suppl 1), 85.
Burstone, C.J., 1962. The biomechanics of tooth movement. In: Kraus, B.S., Riedel, R. A. (Eds.), Vistas in orthodontics: presented to Alton W. Moore. Lea Febiger, Philadelphia, pp. 197–213.
Burstone, C.J., Pryputniewicz, R.J., 1980. Holographic determination of centers of rotation produced by orthodontic forces. Amer. J. Orthodontics 77, 396–409.
Cattaneo, P.M., Dalstra, M., Melsen, B., 2005. The finite element method: a tool to study orthodontic tooth movement. J. Dent. Res. 84, 428–433.
Cattaneo, P.M., Dalstra, M., Melsen, B., 2008. Moment-to-force ratio, center of rotation, and force level: a finite element study predicting their interdependency for simulated orthodontic loading regimens. Am. J. Orthod. Dentofacial Orthoped.: Off. Publ. Am. Assoc. Orthodont Constit. Soc. Am. Board Orthodont. 133, 681–689.
Coolidge, E.D., 1937. The thickness of the human periodontal membrane. J. Am. Dent. Assoc. 24, 260.
Cronau, M., Ihlow, D., Kubein-Meesenburg, D., Fanghänel, J., Dathe, H., Nägerl, H., 2006. Biomechanical features of the periodontium: an experimental pilot study in vivo. Am. J. Orthodont. Dentofacial Orthopedics: Off. Publ. Am. Assoc. Orthodont. Constit. Soc. Am. Board Orthod. 129, 599.
Dalstra, M., Cattaneo, P.M., Beckmann, F., 2006. Synchrotron radiation-based microtomography of alveolar support tissues. Orthod. Craniofac. Res. 9, 199–205.
Dathe, H., Nägerl, H., Kubein-Meesenburg, D., 2013. A caveat concerning center of resistance. J. Dent. Biomech. 4. 1758736013499770.
Dong-Xu, L., Hong-Ning, W., Chun-Ling, W., Hong, L., Ping, S., Xiao, Y., 2011. Modulus of elasticity of human periodontal ligament by optical measurement and numerical simulation. Angle Orthod. 81, 229–236.
Dorow, C., 2004. Numerische Simulation und experimentelle Untersuchung zur Zahnbewegung. Dissertation, Ulm University, Ulm.
Dorow, C., Sander, F.-G., 2005. Development of a model for the simulation of orthodontic load on lower first premolars using the finite element method. J. Orofacial Orthoped/Fortschritte der Kieferorthopädie 66, 208–218.
Garn, S.M., Lewis, A.B., Walenga, A.J., 1968. Maximum-confidence values for the human mesiodistal crown dimension of human teeth. Arch. Oral Biol. 13, 841–844.
Geiger, M.E., Lapatki, B.G., 2014. Locating the center of resistance in individual teeth via two- and three-dimensional radiographic data. J. Orofacial Orthopedics/Fortschritte der Kieferorthopädie 75, 96–106.
Geramy, A., 2000. Alveolar bone resorption and the center of resistance modification (3-D analysis by means of the finite element method). Am. J. Orthod. Dentofac. Orthop. 117, 399–405.
Hohmann, A., Kober, C., Young, P., Dorow, C., Geiger, M., Boryor, A., Sander, F.M., Sander, C., Sander, F.G., 2011. Influence of different modeling strategies for the periodontal ligament on finite element simulation results. Am. J. Orthodont. Dentofacial Orthoped.: Off. Publ. Am. Assoc. Orthodont. Constit. Soc. Am. Board Orthod. 139, 775–783.
Jones, M.L., Hickman, J., Middleton, J., Knox, J., Volp, C., 2001. A validated finite element method study of orthodontic tooth movement in the human subject. J. Orthodont. 28, 29–38.
Keilig, L., Drolshagen, M., Tran, K.L., Hasan, I., Reimann, S., Deschner, J., Brinkmann, K.T., Krause, R., Favino, M., Bourauel, C., 2015. In vivo measurements and numerical analysis of the biomechanical characteristics of the human periodontal ligament. Annals of anatomy = Anatomischer Anzeiger: official organ of the Anatomische Gesellschaft.
Kettenbeil, A., Reimann, S., Reichert, C., Keilig, L., Jäger, A., Bourauel, C., 2013. Numerical simulation and biomechanical analysis of an orthodontically treated periodontally damaged dentition. J. Orofacial Orthopedics/Fortschritte der Kieferorthopädie, 1–14.
Kinney, J.H., Marshall, S.J., Marshall, G.W., 2003. The mechanical properties of human dentin: a critical review and re-evaluation of the dental literature. Crit. Rev. Oral Biol. Med. 14, 13–29.
Kojima, Y., Fukui, H., 2014. A finite element simulation of initial movement, orthodontic movement, and the centre of resistance of the maxillary teeth connected with an archwire. Eur. J. Orthodont. 36, 255–261.
Lapatki, B.G., Paul, O., 2007. Smart brackets for 3D-force-moment measurements in orthodontic research and therapy – developmental status and prospects. J. Orof. Orthoped. Fortschritte der Kieferorthopädie : Organ/Off. J. Deutsche Gesellschaft für Kieferorthopädie 68, 377–396.
Meikle, M.C., 2005. The tissue, cellular, and molecular regulation of orthodontic tooth movement: 100 years after Carl Sandstedt. Eur. J. Orthod. 28, 221–240.
Meyer, B.N., Chen, J., Katona, T.R., 2010. Does the center of resistance depend on the direction of tooth movement? Am. J. Orthod. Dentofacial Orthoped.: Off. Publ. Am. Assoc. Orthodont., Const. Soc. Am. Board Orthodont. 137, 354–361.
Nanci, A., ten Cate, A.R., 2013. Ten Cate's Oral Histology. Development, Structure, and Function. Elsevier, St, Louis, Mo.
Natali, A.N., Carniel, E.L., Pavan, P.G., Sander, F.G., Dorow, C., Geiger, M., 2008. A visco-hyperelastic-damage constitutive model for the analysis of the

biomechanical response of the periodontal ligament. J. Biomech. Eng. 130, 31004.
Nikolaus, A., Currey, J.D., Lindtner, T., Fleck, C., Zaslansky, P., 2017. Importance of the variable periodontal ligament geometry for whole tooth mechanical function. A validated numerical study. J. Mech. Behav. Biomed. Mater. 67, 61–73.
Nyashin, Y., Nyashin, M., Osipenko, M., Lokhov, V., Dubinin, A., Rammerstorfer, F., Zhurov, A., 2015. Centre of resistance and centre of rotation of a tooth. Experimental determination, computer simulation and the effect of tissue nonlinearity. Comput. Methods Biomech. Biomed. Eng. 19, 229–239.
O'Mahony, A.M., Williams, J.L., Spencer, P., 2001. Anisotropic elasticity of cortical and cancellous bone in the posterior mandible increases peri-implant stress and strain under oblique loading. Clin. Oral Implant Res. 12, 648–657.
Osipenko, M.A., Nyashin, M.Y., Nyashin, Y.I., 1999. Center of resistance and center of rotation of a tooth. The definitions, conditions of existence, properties. Russ. J. Biomech. 1999, 5–15.
Papadopoulou, K., Hasan, I., Keilig, L., Reimann, S., Eliades, T., Jäger, A., Deschner, J., Bourauel, C., 2013. Biomechanical time dependency of the periodontal ligament: a combined experimental and numerical approach. Eur. J. Orthod.
Peck, H., Peck, S., 1972. An index for assessing tooth shape deviations as applied to the mandibular incisors. Am. J. Orthodont. 61, 384–401.
Poppe, M., Bourauel, C., Jäger, A., 2002. Determination of the elasticity parameters of the human periodontal ligament and the location of the center of resistance of single-rooted teeth a study of autopsy specimens and their conversion into finite element models. J. Orofacial Orthopedics = Fortschritte der Kieferorthopädie : Organ/Off. J. Deutsche Gesellschaft für Kieferorthopädie 63, 358–370.
Provatidis, C.G., 1999. Numerical estimation of the centres of rotation and resistance in orthodontic tooth movement. Comput. Methods Biomech. Biomed. Eng. 2, 149–156.
Provatidis, C.G., 2000. A comparative FEM-study of tooth mobility using isotropic and anisotropic models of the periodontal ligament. Med. Eng. Phys. 22, 359–370.
Qian, H., Chen, J., Katona, T.R., 2001. The influence of PDL principal fibers in a 3-dimensional analysis of orthodontic tooth movement. Am. J. Orthod. Dentofacial Orthoped.: Off. Publ. Am. Assoc. Orthodont. Constit. Soc. Am. Board Orthodont. 120, 272–279.
Schmidt, F., Kilic, F., Piro, N.E., Geiger, M.E., Lapatki, B.G., 2018. Novel method for superposing 3D digital models for monitoring orthodontic tooth movement. Ann. Biomed. Eng. 46, 1160–1172.
Schumacher, G.-H. (Ed.), 1983. Anatomie und Biochemie der Zähne. Verl. Volk und Gesundheit, Berlin.
Schwartz-Dabney, C.l., Dechow, P.c., 2003. Variations in cortical material properties throughout the human dentate mandible. Am. J. Phys. Anthropol. 120, 252–277.
Tanne, K., Koenig, H.A., Burstone, C.J., 1988. Moment to force ratios and the center of rotation. Am. J. Orthod. Dentofac. Orthop. 94, 426–431.
Toms, S.R., Eberhardt, A.W., 2003. A nonlinear finite element analysis of the periodontal ligament under orthodontic tooth loading. Am. J. Orthod. Dentofac. Orthop. 123, 657–665.
Towfighi, P.P., Brunsvold, M.A., Storey, A.T., Arnold, R.M., Willman, D.E., McMahan, C.A., 1997. Pathologic migration of anterior teeth in patients with moderate to severe periodontitis. J. Periodontol. 68, 967–972.
Viecilli, R.F., Budiman, A., Burstone, C.J., 2013. Axes of resistance for tooth movement: does the center of resistance exist in 3-dimensional space? Am. J. Orthod. Dentofac. Orthop. 143, 163–172.
Vollmer, D., Bourauel, C., Maier, K., Jäger, A., 1999. Determination of the centre of resistance in an upper human canine and idealized tooth model. Eur. J. Orthodont. 21, 633–648.
Yoshida, N., Koga, Y., Kobayashi, K., Yamada, Y., Yoneda, T., 2000. A new method for qualitative and quantitative evaluation of tooth displacement under the application of orthodontic forces using magnetic sensors. Med. Eng. Phys. 22, 293–300.
Yoshida, N., Koga, Y., Peng, C.-L., Tanaka, E., Kobayashi, K., 2001. In vivo measurement of the elastic modulus of the human periodontal ligament. Med. Eng. Phys. 23, 567–572.
Zhurov, A.I., Limbert, G., Aeschlimann, D.P., Middleton, J., 2007. A constitutive model for the periodontal ligament as a compressible transversely isotropic visco-hyperelastic tissue. Comput. Methods Biomech. Biomed. Eng. 10, 223–235.